JOURNAL OF SPACECRAFT AND ROCKETS
Vol. 46, No. 5, September–October 2009

Spacecraft Radiation Shielding Using Ultralightweight Superconducting Magnets

Erwan A. Kervendal* and Daniel R. Kirk†
Florida Institute of Technology, Melbourne, Florida 32901
and
Reiner B. Meinke‡
Advanced Magnet Laboratory, Inc., Palm Bay, Florida 32905

DOI: 10.2514/1.37490

This work examines the performance and feasibility of a novel inflatable lightweight spacecraft radiation shielding system employing superconducting magnet technology. In the proposed approach a set of lightweight toroid-shaped coils surround a spacecraft creating strong shielding fields, which are wholly contained within the volume of the coils, leaving the spaceship free of magnetic fields. A numerical model and Monte Carlo optimization tool were developed to simulate the interaction of ionizing particles with various confined magnetic field configurations and geometries. Using an isotropic distribution of protons with kinetic energies ranging from 0.1 to 2 GeV, the model was used to explore a wide parametric space of potential spacecraft shielding options and to assess which parameters are most responsible for determining shielding effectiveness. For a candidate spacecraft, it was found that more than 90% of incident particles with a 1-GeV kinetic energy could be deflected away from the spacecraft using a 5-T toroid-shaped shield.

Nomenclature

a	=	radius of the wire loop, m
B	=	magnetic field intensity, T
B_r	=	radial component of the magnetic field, T
B_z	=	axial component of the magnetic field, T
c	=	speed of light, 299,792,458, m/s
E_k	=	kinetic energy of particles, eV
E_0	=	energy of particles at rest, eV
F	=	Lorentz force, N
I	=	current in conductors, A
m	=	relativistic mass, kg
m_0	=	rest mass, kg
N	=	number of conductor turns
N_{OFF}	=	number of particles that hit the spacecraft when there is no shield
N_{ON}	=	number of particles that hit the spacecraft when the shield is active
p	=	particle momentum, GeV/c
q	=	charge of particle, C
r	=	radial distance from the center of the toroid, m
V	=	velocity of particle, m/s
η	=	efficiency
μ_0	=	vacuum permeability, $4\pi \times 10^{-7}$, V T m/A
ρ	=	radius, m
φ	=	azimuthal direction

I. Introduction

SPACECRAFT carrying human missions to Mars will be exposed to ionizing radiation for extended periods of time. Exposure of the crew and instrumentation to such radiation must be minimized. Hazardous radiation may originate from the sun in the form of solar wind or flare-ups, or may be in the form of high-energy galactic radiation which pervades the solar system. Althogh low-energy particles may be absorbed by spaceship walls, higher momentum particles (>100 MeV/c) require heavy shielding with thicknesses of up to several centimeters for absorption [1–4]. Alternative low-mass shielding methods would benefit space missions by reducing the gross liftoff weight. Recent advances in high-temperature superconductors and magnet technology suggest the possibility of using high-strength magnetic fields to repel charged particles over a wide energy range. In the proposed approach a set of lightweight toroid-shaped coils surround a spacecraft creating strong shielding fields, which are wholly contained within the volume of the coils, leaving the spaceship free of magnetic fields. A mathematical model was developed to predict the ability of the shield to repel high kinetic energy particles away from the spacecraft. The tool was then used to optimize the design of a radiation shielding system for a spacecraft approximately sized for a human mission to Mars. Protecting the spacecraft using the proposed system would improve safety while minimizing the considerable mass penalty associated with an equally effective passive shielding approach.

Presented as Paper 0497 at the AIAA Aerospace Sciences Meeting, Reno, NV, 8–11 January 2007; received 11 March 2008; revision received 24 April 2009; accepted for publication 28 April 2009. Copyright © 2009 by the American Institute of Aeronautics and Astronautics, Inc. All rights reserved. Copies of this paper may be made for personal or internal use, on condition that the copier pay the $10.00 per-copy fee to the Copyright Clearance Center, Inc., 222 Rosewood Drive, Danvers, MA 01923; include the code 0022-4650/09 and $10.00 in correspondence with the CCC.

*Graduate Research Assistant, Mechanical and Aerospace Engineering Department. Student Member AIAA.
†Associate Professor, Mechanical and Aerospace Engineering Department. Senior Member AIAA.
‡President.

II. Superconducting Magnetic Shield Concept

This section presents an overview of the superconducting magnetic shielding concept, as well as basic design parameters and operation of the shielding system in a space environment.

A. Lorentz Force and Toroidal Magnetic Fields

In the same way that prisms and lenses are used to bend, focus, or defocus light rays, charged particle trajectories are affected by magnetic fields due to the Lorentz force which is mutually perpendicular to the direction of particle motion and the magnetic field, as shown in Eq. (1):

$$\mathbf{F} = q \cdot (\mathbf{V} \times \mathbf{B}) \tag{1}$$

Because the particle energy, charge, and velocity are not altered by static magnetic fields they are independent of the shielding design. To deflect particles away from the spacecraft, forces must be large and are set by the magnetic field intensity B according to Eq. (1). For example, if a charged particle moves in a constant magnetic field, its

trajectory becomes a circle with radius ρ, where q is in units of electron charge, the particle momentum p is in units of GeV$/c$ and B is in Tesla, as shown in Eq. (2):

$$\rho = q \cdot \frac{p}{0.3B} \tag{2}$$

Using Eq. (2), a proton of 1 GeV$/c$ in a magnetic field of 1 T has a bending radius of 3.3 m. This illustrates that particles may be significantly deflected over a distance of a few meters using magnetic fields of around 1 T.

The coil geometry shown in Fig. 1 represents a toroid, responsible for creating the toroidal magnetic field.

The conductor is wrapped around a donut-shaped coil former, and to a good approximation the field is completely contained inside the coil and the field lines form concentric circles. Assuming that the field is generated by infinitely thin currents flowing on the outer toroidal surface, the field is only in the circumferential direction. Ideally, the strength of the field B is given by Eq. (3):

$$\mathbf{B} = B(r) \cdot \boldsymbol{\varphi} = \frac{\mu_0 \cdot N \cdot I}{2\pi \cdot r} \cdot \boldsymbol{\varphi} \tag{3}$$

The fact that the field is wholly contained within the toroid is of great importance to the space shield application. The spaceship can be located on the inside of the toroid, as shown in Fig. 2, where the field is ideally zero and spacecraft operation is not influenced by the shielding fields.

B. Operation of Superconducting Coils in Space

High-temperature superconductors like bismuth lead strontium, calcium copper oxygen (BSCCO) and yttrium barium copper oxide (YBCO) allow operation of the conductor at high currents and high magnetic fields at the temperatures of liquid hydrogen (~20 K) or even higher. Operating superconducting magnets in interplanetary space has significant advantages over operation on Earth, where the superconducting coil needs to be well insulated to avoid excessive heat loads. The insulation required on the Earth has to reject thermal radiation (depending on surrounding temperature), gas convection (requiring vacuum insulation), and finally thermal conduction (depending on the mechanical support structure of the superconducting coil and the ambient temperature). The low particle density in interplanetary space eliminates gas convection as a source of heating and the necessity of an extra vacuum vessel surrounding the superconducting coil. Because of the low ambient temperature in space, heating of the superconducting coil can only result from absorbed radiation from the sun and energy deposition of absorbed cosmic ray particles. Placing solar panels in front of the superconducting coils would largely eliminate photon radiation as the heat source. The remaining relatively low heat load on the magnets can be accommodated by cryocoolers, which have already been successfully used on a number of satellites, such as NASA's solar-flare-studying satellite RHESS. Given the advantages of the space environment, the thermal containment of the superconducting magnet could be very simple and lightweight.

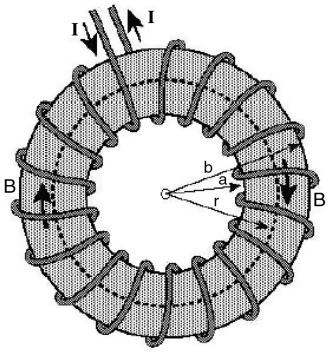

Fig. 1 Schematic of a toroidal coil layout.

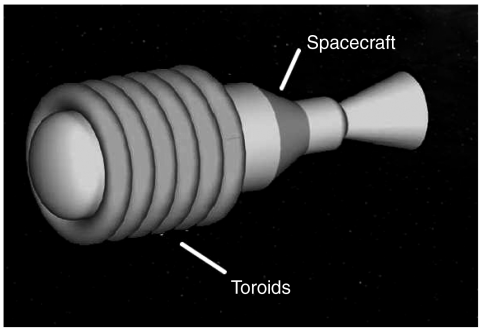

Fig. 2 Shielding system surrounding a spacecraft.

The superconducting coils would be operated in a persistent mode, meaning no current attenuation for the operational time should be observed. The coils would be charged while in space, and typical currents for the required fields would be in the range of 10,000 A. Powered by solar energy and using a flux pump such currents can be built up without using a high-current power supply, and a charging time of about one day is required.

C. Superconducting Coil Design: Self-Inflating, Energy Storage, and Flux Pumping

To reduce the mass inherent to passive magnetic shields, such as the concept investigated by Hoffman et al. [5], structural support for the toroids is based on inflatable space modules. Investigated by NASA [6] in the 1960s, inflatable structures are currently under development for space stations. The proposed concept is based on a basic donut-shaped support structure, made like a balloon, and consisting of a strong, fiber reinforced, lightweight support material like that used by Bigelow Aerospace as a follow-up to NASA's TransHab inflatable module concept [7]. To create the shield, a high-temperature superconductor is attached to the balloon surface. Existing superconductors are in tape form, where the superconducting material forms a flexible layer with a thickness of about 10 μm. It is proposed to form the helical conductor path for the toroidal coils using a similar approach. As in existing tape conductors the superconductor has a backing of a high conductivity material like silver or aluminum for stabilization.

Unlike inflatable space modules, the balloon support structures of the proposed magnets are self-inflating under the effect of the acting Lorentz forces of the superconducting coil. The forces in such helical windings act like internal pressure caused by the magnetic field, as described in Eq. (4):

$$P_{\text{magnetic}} = \frac{B^2}{2\mu_0} \tag{4}$$

Because of the self-inflating property of the magnet support structure, leak tightness of the balloon is not essential and no extra shield is needed for absorbing micrometeorites, which may punch tiny holes into the structure. It is also conceivable to use a support structure like a mesh that is made out of high-strength fibers to further reduce weight. An additional advantage is the significant amount of energy stored by the magnet, which can be estimated by assuming an average field in the magnets and the volume of toroidal coils through Eq. (5):

$$E_{\text{stored}} = \frac{B^2_{\text{average}}}{2\mu_0} \cdot \text{volume} \tag{5}$$

For example, the stored energy is about 0.4 MJ$/$m3 for a magnetic field of 1 T. Part of this energy could be extracted if needed, for example, as emergency power or to operate an auxiliary thruster.

A flux pump is based on superconductivity and flux trapping, as illustrated in Fig. 3.

Using a permanent magnet with a periodic motion, a flux can be introduced through a low pinning force material generating a low superconducting field. Therefore, a flux can penetrate the superconductor. The latter being superconductive, the flux is locally

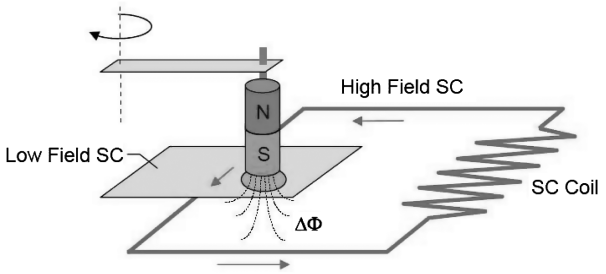

Fig. 3 Flux pump operational schematic. SC = superconducting.

trapped and introduced into the superconducting coil. The purpose of such a motion is the induction of a very high-current density. In fact, the motion of the flux inside the superconductor induces a voltage and increases the current into the coil. After many flux motions into the superconducting coil, consistent current flows through the coil, and a high magnetic field can be provided. The primary advantage of such a device is that significant currents can be induced into the superconducting coil with minimal energy requirements through use of a permanent magnet. A toroidal magnetic field used along with a flux pump enables the design of an efficient, reasonably sized, active shielding system.

A unique feature of the proposed shielding system is its relatively low weight and that the shielding material is only a small fraction of an interaction length in thickness. In comparison to any passive shielding material the proposed system has a much lower probability of generating secondary particle showers triggered by an interaction of a primary incoming particle. Furthermore, it is important to consider the energy spectrum of the incoming particles. There are cosmic ray particles with extremely high energies, which cannot be stopped by any shielding method. Because such particles cannot be stopped or deflected, the best method of mitigating their effect is by reducing their interaction probability, as is done in the proposed design. With a passive system the probability of a secondary shower is strongly enhanced and many of the produced secondary particles will enhance detrimental effects. Incoming primary particles with low energy will mainly produce pions, which rapidly decay. Their decay products will have very low energies which will be curled up in the magnetic field and absorbed with little or no effect on the material of the shield.

Radiation damage of the materials proposed for the active superconducting shields is a minor problem. Although little or no data are currently available for the ultimate radiation hardness of high-temperature superconductors (HTS), it is safe to assume that the ionizing particle flux experienced in space is well below the limit where HTS conductors are adversely affected. Studies already performed with HTS materials indicate that the critical current density of these materials actually increases with irradiation of ionizing particles. This is due to the fact that pinning centers are needed to "harden" superconductors and such pinning centers can be produced by inclusions or dislocation in the base material. Furthermore, HTS materials are under consideration for accelerator applications, where extremely high radiation levels cause actual heating and quenching of conductors. Metallic low temperature superconductors (LTS) with their extremely high radiation hardness are not applicable because their energy margin to quenching is too low. Because of the relatively high critical temperatures of HTS conductors, like YBCO, their energy margin is more than 1000 times larger than LTS materials like NbTi.

III. Computational Model

This section discusses the development of a numerical model for simulating various magnetic shielding configurations. The interaction and shielding efficiency of high-energy particles with the shield system are studied and the most important performance parameters are identified.

A. Particles Distribution

The distribution of solar wind is essentially isotropic in interplanetary space [8], and protons with kinetic energies and frequency of occurrence from 0.1 to 1 GeV have been identified as most hazardous for spacecraft traveling in the solar system [8–16]. Consequently, an isotropic distribution of protons with kinetic energies from 0.1 to 2 GeV was investigated and velocity values were randomly computed from the kinetic energy E_k, according to Eq. (6):

$$\left(\frac{V}{c}\right) = 1 - \frac{1}{(1 + E_k/E_0)^2} \tag{6}$$

The simulated particles have velocities that approach the speed of light. By requiring the conservation of mass and momentum to be invariant in Lorentz transformations, the relation between the rest mass of the body m_0 and that of the same body at a given velocity v is given by the special relativity relation of Eq. (7):

$$m = \frac{m_0}{(1 - v^2/c^2)^{1/2}} \tag{7}$$

As long as the particle is outside the magnetic field of the toroid, its trajectory is a straight line because there are no applied forces (interactions between particles or the gravitational force due to Earth or other planets are neglected). As static magnetic fields do not accelerate or decelerate particles, but only bend the particle's trajectory, the total velocity of the particle does not change as it travels through the magnetic field; consequently mass remains constant.

The initial positions of the particles are created on the surface of a sphere which has a radius large enough with respect to the spacecraft to simulate a homogeneous, isotropic distribution, as illustrated in Fig. 4.

B. Magnetic Field Computation

The deviation between the ideal magnetic field strength, as given by Eq. (3), and the actual magnetic field strength generated by a filament in which a current flows was assessed. The magnetic field generated by one thin current carrying wire filament is given by Eq. (8), where K and E are elliptical integrals of the first and second kinds, respectively [17], given by Eq. (9), and r and z are the polar coordinates of any point in space where the magnetic field is calculated as illustrated in Fig. 5 and the results are shown in Fig. 6:

$$\begin{aligned} B_r(r,z,a) &= \frac{I\mu_0}{2\pi} \cdot \frac{z}{r\sqrt{(r+a)^2+z^2}} \\ &\quad \cdot \left[K(r,z,a) - \frac{(r^2+a^2+z^2)}{(r-a)^2+z^2} \cdot E(r,z,a) \right] \\ B_z(r,z,a) &= \frac{I\mu_0}{2\pi} \cdot \frac{1}{\sqrt{(r+a)^2+z^2}} \\ &\quad \cdot \left[K(r,z,a) - \frac{(r^2-a^2+z^2)}{(r-a)^2+z^2} \cdot E(r,z,a) \right] \end{aligned} \tag{8}$$

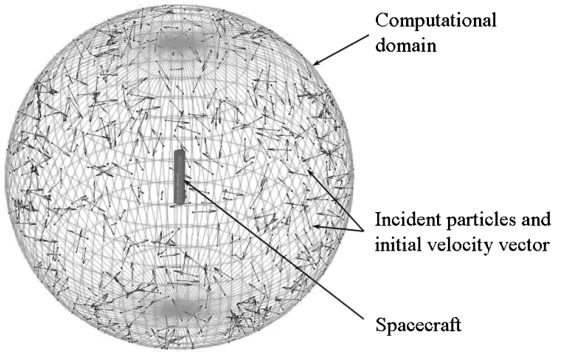

Fig. 4 Computational domain and vectors depicting initial particle distribution and velocity.

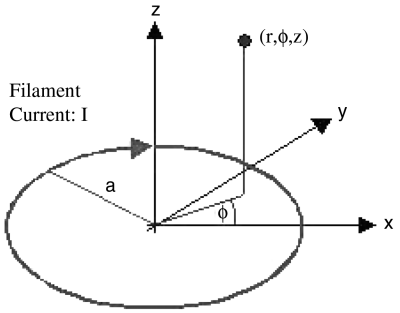

Fig. 5 Thin wire loop with current I.

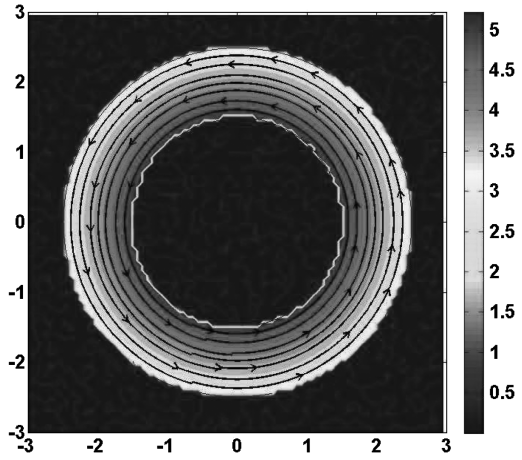

Fig. 6 Toroidal magnetic field lines and magnitude.

$$K(r,z,a) = \int_0^{\pi/2} \left[1 - \frac{4ar}{(r+a)^2 + z^2} \cdot \sin\theta\right]^{-1/2} \mathrm{d}\theta$$

$$E(r,z,a) = \int_0^{\pi/2} \left[1 - \frac{4ar}{(r+a)^2 + z^2} \cdot \sin\theta\right]^{1/2} \mathrm{d}\theta \qquad (9)$$

Using thin filaments simulated every 0.5 deg with grid size of 10^{-3} m, a comparison between the magnetic field intensities as computed using Eqs. (8) and (9) versus the simplified Eq. (3) was performed. Within the toroid the difference is on the order of 10^{-6} T when the maximum magnetic field intensity is set to 5 T. Based on this level of agreement, it was decided to use Eq. (3) for magnetic field computation within the toroid and to set the field strength to zero outside the shield. These approximations are appropriate for this study for several reasons. By comparing the maximum field intensity inside (5 T) and outside the toroid (on the order of 10^{-2} to 10^{-5} T within a few centimeters of the toroid as predicted using Eqs. (8) and (9)), it may be shown, using Eq. (2), that the external magnetic field has little effect on the particles' motion as compared to within the torus. Next, the calculation of magnetic field based on Eqs. (8) and (9) is very CPU demanding and is not an efficient means of performing extensive Monte Carlo simulations to perform a preliminary optimization of the shield design. Finally, to accurately model the external magnetic field within a few centimeters of the toroid, a detailed model would require consideration of the effect of helical windings around the torus and the associated local peaks in magnetic intensity near the wires. This effect was neglected based on the ratio of a typical dimension of the windings (several centimeters) as compared to the overall toroid size (several meters). These issues could be addressed in future work with an emphasis on magnetic field computation and interaction with toroid materials. Such a model would be especially useful to examine the detailed performance of the optimized shield design identified using the simplified Monte Carlo simulation tool employing Eq. (3).

C. Shielding Efficiency and Time-Step Criteria

To characterize the performance of a given shielding configuration, an expression for efficiency was developed. The efficiency compares the number of particles that would hit the spacecraft without shielding, N_{OFF}, to the number of particles that hit the spacecraft when the shield is turned on, N_{ON}. The same set of particles (position and velocity), as shown in Fig. 4, was used to derive these two quantities. The efficiency is defined in Eq. (10):

$$\eta = 1 - \frac{N_{\mathrm{ON}}}{N_{\mathrm{OFF}}} \qquad (10)$$

To compute the three-dimensional trajectory of each particle an explicit fifth-order accuracy Runge–Kutta scheme was used to solve Newton's second law with the Lorentz force as the only acting force; calculations use the Lorentz force as defined in Eq. (1), particle mass is calculated from Eq. (7), and the magnetic field is given by Eq. (3). Two different domains of computation were defined. Based on the discussion of Sec. III.B, the magnetic field is taken as zero as long as the particle is outside the toroid. Therefore, no force acts on particles and no change in motion occurs. For the sake of CPU-time reduction, the time step could be taken as a large value until the particle impacts the toroid. The time-step approach is different for the trajectory computation within the torus. Within the shield, the time step was set to be small enough to be representative of typical particle motions, including possible gyromotion. According to Vogt [18], for a proton with a kinetic energy of 2 GeV within a uniform magnetic field of 5 T, the gyroperiod is about 1.3×10^{-8} s and the gyroradius is about 0.5 m. Consequently, the time-step approach consisted of initializing the step in time as a function of kinetic energy and distance from the toroid's center. For example, the time step was initially set to 6×10^{-9} s/10 (the factor 1/10 to be additionally conservative) for a 2 GeV proton entering a toroid with 1.5 m diameter. The time step was then reduced as the particle moved closer to the center of the toroid, resulting in a time step of 2×10^{-9} s/10 at 0.5 m from the center. This is because as the particles get closer to the center of the toroid the magnetic field strength increases which more significantly alters the particles' trajectory requiring a smaller time step to accurately resolve the motion. In the Monte Carlo simulations gyromotions were only observed for a few limited combinations of incident particle velocity and approach angle to the spacecraft.

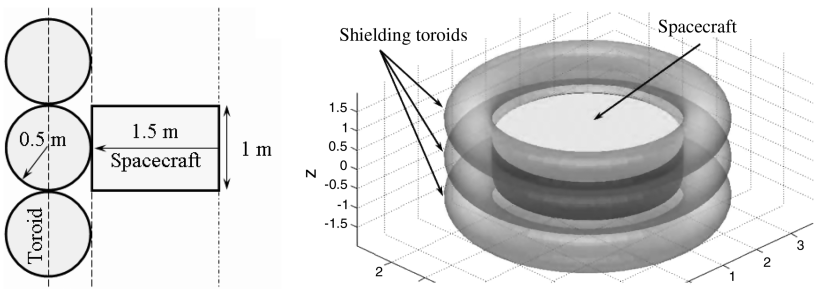

a) b)

Fig. 7 a) Spacecraft slice and three toroidal shields. b) 3-m-diam and 1-m-height spacecraft slice protected by three toroids with diameter 1 m.

IV. Results and Discussion

To assess the effectiveness of the shielding concept, a cylindrically shaped spacecraft 9 m long and 3 m in diameter was selected as a case study. Before attempting to protect the entire spacecraft, a 1-m-long slice of the spacecraft was first studied as shown in Figs. 7a and 7b.

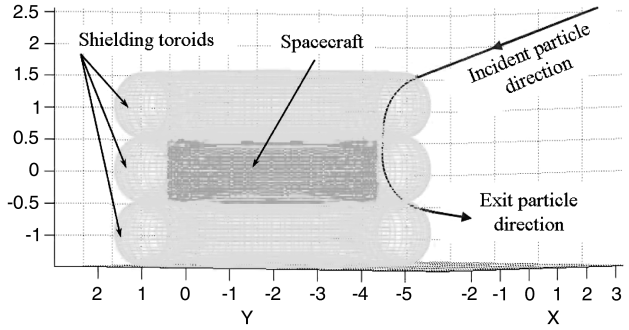

Fig. 8 Example of a 1 GeV particle deflected away from the spacecraft due to the presence of a 5-T peak magnetic field in each toroid.

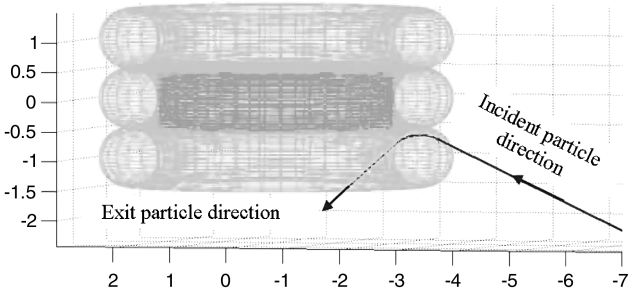

Fig. 9 Example of a 1 GeV particle deflected away from the spacecraft due to the presence of a 5-T peak magnetic field in each toroid.

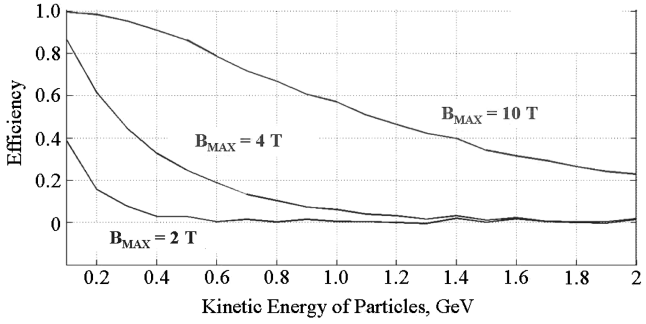

Fig. 10 Efficiency vs particle kinetic energy for 10,000 particles and $R = 0.5$ m.

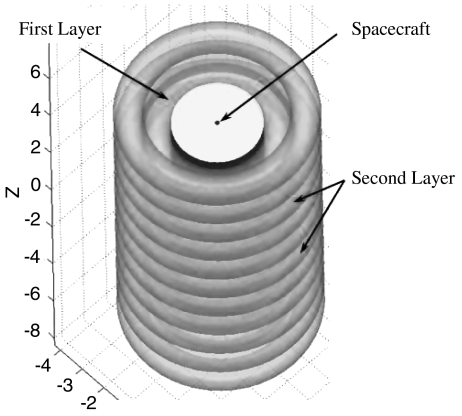

Fig. 12 Optimized spacecraft shielding configuration featuring two layers of toroids and one layer of embedded toroids.

In all toroidal configurations investigated, the inner diameter of the toroidal ring is equal to the outer diameter of the spacecraft, or 3 m in Fig. 7. In the case of the spacecraft slice investigation, the toroid diameter is equal to the height of a spacecraft slice (1 m in Fig. 7). The central toroid is aligned adjacent to the slice and is expected to do most of the shielding. Two additional toroids were included to simulate the effects that contiguous toroids have on the incident radiation. An example of how energetic particles are deflected due to the presence of the magnetic fields is shown in Figs. 8 and 9. For these figures, the peak magnetic field strength is set to 5 T and the incident particle has a kinetic energy of 1 GeV.

In Figs. 8 and 9, if the shields were not present, or the magnetic field turned off, the incident particles would strike the cylindrical portion of the spacecraft. However, when the shields are turned on, the same particles which would have struck the spacecraft are now deflected safely away from the spacecraft.

The efficiency of the shielding system as a function of the magnetic field strength using the geometry of Fig. 7 was investigated. Five simulations of 10,000 particles each with random initial positions and kinetic energies over a range of 0.1–2 GeV were averaged, and the result of this Monte Carlo simulation is summarized in Fig. 10.

For a maximum field strength of 2 T the efficiency is 40% for 0.1 GeV particles and 5% for energies above 1 GeV. For a value of 4 T, the efficiency improves to 85% at 0.1 GeV but still decreases to around 5% for kinetic energies beyond 1 GeV. The efficiency can be significantly improved for a magnetic field strength of 10 T to 99% at 0.1 GeV, 58% at 1 GeV, and 22% at 2 GeV. Increasing the strength of the peak magnetic field from 2 to 10 T improves shielding efficiency for incident particles with energies from 0.1 to 2 GeV. Such simulations demonstrate the potential benefits that the proposed shielding system may provide.

Upon completion of the spacecraft slice study, other geometric shielding configurations, including varying the dimensions of the

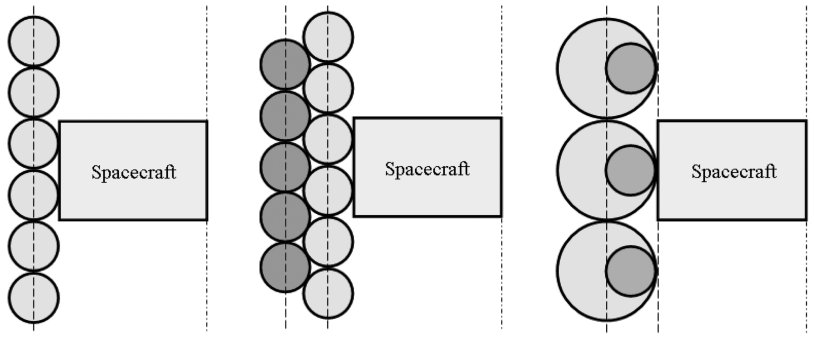

Fig. 11 a) Various toroid configurations investigated: varying geometry and number of toroids. b) Various toroid configurations investigated: layers of toroids. c) Various toroid configurations investigated: embedded toroid concept.

Table 1 Efficiency of various toroidal shielding configurations at 0.1, 1, and 2 GeV

Shielding geometry description	0.1 GeV	1 GeV	2 GeV
Layer 1 only	99.9%	55%	26%
Layers 1 and 2 only	99.9%	82%	51%
Layer 1, layer 2, and embedded toroids in layer 1	99.8%	89%	57%

toroids, employing multiple layers of toroids and toroids embedded within toroids, as shown in Figs. 11a–11c, were examined as ways to further increase the efficiency of the shielding system.

Since the particles' trajectory within a toroid is always deflected in the same direction, the embedded toroid concept was introduced as an efficient means to increase locally the intensity of the magnetic field where it is needed. These configurations were also examined to determine the tradeoff between the geometric configuration of the shielding system and the maximum magnetic field strength required to achieve a given level of shielding efficiency.

After developing an understanding of the effectiveness of these basic shielding options, an entire candidate spacecraft was simulated. For a maximum magnetic field of 5 T, an optimized spacecraft shielding system, which makes use of a double layer of toroids and embedded toroids, was identified using the Monte Carlo simulation tool. The configuration of the toroids surrounding the sides of the spacecraft is shown in Fig. 12; the performance as a function of incident radiation energy is summarized in Table 1 and shown in Fig. 13.

Shielding configuration and dimensions are as follows:

1) *all layers* at 5 T maximum strength;

2) *layer 1*: 10 toroids with height of 3 m and diameter of 1.5 m each;

3) *layer 2*: the second layer is made up of 11 toroids with a height of 3 m and a diameter of 7.5 m;

4) *embedded toroids*: the embedded toroids are introduced in layer 1.

The optimized spacecraft shielding system shows that for 0.1 GeV particles, a single layer of toroids at 5 T is sufficient to block 99.9% of the incident radiation. For 1 GeV particles, however, the single layer system only deflects 55% of the incident radiation. The addition of a second layer of toroids increases the shielding efficiency to 82%, and the addition of a second layer along with embedded toroids in the first layer increases the shielding efficiency to 89% for the 1 GeV particles. Finally, a shielding effectiveness of 57% can be achieved for 2 GeV particles using a shielding concept of two layers with embedded toroids in the first layer. Such a shielding configuration represents over a 100% improvement above the single layer configuration.

The simulations do not include the effect of a cap portion at the front and back ends of the spacecraft, but rather focused exclusively on developing an optimized toroidal shielding configuration to protect the cylindrical sides of the spacecraft, which for this geometry comprised 86% of the exposed surface area. To protect the ends of the spacecraft, a combination of active and passive shielding techniques could be employed. For example, a series of several toroids with diminishing diameter could be nested coaxially on the ends of the spacecraft to cover most of the exposed area. When the toroids reduce to a size that is impracticably small, the final central area could be protected with an increase in spacecraft wall thickness. Regardless of the strategy to protect the end caps of the spacecraft, for a majority of the surface area the active magnetic toroid shields are a very attractive option.

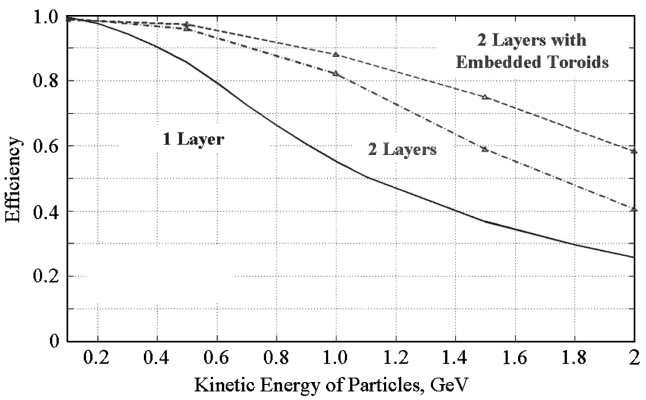

Fig. 13 Efficiency predictions for shielding of an entire spacecraft using various shielding concepts.

V. Conclusions

This paper discussed a new inflatable superconducting magnetic shielding system to protect spacecraft from radiation. Using an ultralightweight structure and innovative power supply, a magnetic field of great strength can be created to surround a spacecraft and deflect ionizing particles, which may be hazardous for both crew health and onboard electronics. A mathematical model and Monte Carlo simulation tool were developed to predict the ability of any magnetic shielding configuration to deflect dangerous particles award from the spacecraft. The specific conclusions of this study are as follows:

1) Using superconducting magnet technology to produce field strengths of several Tesla, significant deflection of charged particles in the 0.1–2 GeV energy range occurs over a distance of a few meters which is practical for spacecraft shielding applications.

2) A combination of layered and embedded toroids greatly enhances the deflection capabilities of a candidate shielding system. With a maximum magnetic field strength of 5 T, the system can be used to protect a spacecraft with a shielding efficiency of about 90% for particles in the 1 GeV range, and an efficiency of 57% for particles in the 2 GeV range.

3) The lightweight, self-inflating shielding system is not sensitive to micrometeorite impacts and may be used for auxiliary energy storage. The superconducting layer on the surface of the toroids constitutes a small fraction of an interaction length and relative to passive shields has a much lower probability of generating secondary particle showers triggered by an interaction of a primary incoming particle.

Current work is focused on coupling the simulation tool with a CAD package which will allow an optimized shielding system for a spacecraft of any dimensions and shape to be developed.

References

[1] Wilson, J. W., Cucinotta, F. A., Kim, M. -H. Y., and Schimmerling, W., "Improved Spacecraft Materials for Radiation Protection: Shield Materials Optimization and Testing," *First International Workshop on Space Radiation Research and Eleventh Annual NASA Space Radiation Health Investigators' Workshop*, Arona, Italy, 27–31 May 2000, *Physica Medica*, Vol XVII, Supplement 1, 2001.

[2] Wilson, J. W., Cucinotta, F. A., Miller, J., Shinn, J. L., Thibeault, S. A., Singleterry, R. C., Simonsen, L. C., and Kim, M. -H. Y., "Materials for Shielding Astronauts from the Hazards of Space Radiation," *Materials Research Society Symposium Proceedings*, Vol. 551, 1999, pp. 3–15.

[3] Wilson, J. W., Miller, J., Konradi, A., and Cucinotta, F. A., "Shielding Strategies for Human Space Exploration," *NASA Conference Publication 3360*, 1997.

[4] Townsend, L. W., "Overview of Active Methods for Shielding Spacecraft from Energetic Space Radiation," *11th Annual NASA Space Radiation Health Investigators' Workshop*, 27–31 May 2000.

[5] Hoffman, J. A., Fisher, P., and Batishchev, O., "Use of Superconducting Magnet Technology for Astronaut Radiation Protection," NIAC Phase 1 Final Rept. CP 04-01 2005.

[6] Keffer, C. O., "Experimental Investigation of Packaging and Deployment Characteristics of an Inflatable Toroidal-Space Station Configuration," NASA TM-X-1079, April 1965.

[7] Covault, C., "Inside the Bigelow Inflatable-Module Plant," *Aviation Week & Space Technology*, 26 Sept. 2004.

[8] Spillantini, P., Taccetti, F., Papini, P., Rossi, L., and Casolino, M., "Radiation Shielding of Astronauts in Interplanetary Flights: The CREAM Surveyor to Mars and the Magnetic Lens for a Spaceship,"

Physica Medica, Vol 17, Suppl. 1, 2001, pp. 249–254.

[9] Stone, E. C., Frandsen, A. M., Mewaldt, R. A., Christian, E. R., Margolies, D., Ormes, J. F., and Snow, F., "Advanced Composition Explorer," *Space Science Reviews*, Kluwer, Dordrecht, The Netherlands, 1998 http://www.srl.caltech.edu/ACE.

[10] Newman, D., "Space Environment and Its Interaction with Space Travelers," *Space Biomedical Engineering and Life Support*, Massachusetts Institute of Technology, Cambridge, MA, 2009.

[11] Mewaldt, R. A., "Cosmic Rays," *Macmillian Encyclopedia of Physics*, Macmillan, New York, 1996.

[12] Anon., "Gravitation, Cosmology, and Cosmic-Ray Physics: A Research Briefing, Board on Physics and Astronomy Commission on Physical Sciences," Mathematics and Applications National Research Council, National Academy Press, Washington, D.C., 1994.

[13] Nymmik, R. A., "Behavioural Features of Energy Spectra of Particle Fluences and Peak Flux in Solar Cosmic Rays," *Proceedings of the 24th International Cosmic Ray Conference*, Roma, Vol. 3, 1995, pp. 66.

[14] "Cosmic Ray Effects on Microelectronics, Part 4," NRL Memorandum Rept. 5901, 1986 and "Cosmic Ray Effects on Microelectronics, Part 1: Near-Earth Particle Environment," NRL Memorandum Rept. 4506, 1981.

[15] Badhwar, G. D. and O'Neil, P. M., "Galactic Cosmic Radiation Model and its Applications," *Advances in Space Research*, Vol. 17, No. 2, 1996, pp. 7–17. doi:10.1016/0273-1177(95)00507-B

[16] Wilson, J. W., Cucinotta, F.A., Tai, H., Simonsen, L.C., Shinn, J.L., Thibeault, S., and Kim, M.Y., "Galactic and Solar Cosmic Ray Shielding in Deep Space," NASA TR 3682, Dec. 1997.

[17] Thoem, R. J. and Tarrh, J. M., "Field and Force Design Concepts," *MHD and Fusion magnets*, John Wiley & Sons Canada, Ltd., New York, 1982.

[18] Vogt, J., "Lecture on Radiation Belts," *General Geosciences and Astrophysics Space Physics Module*, International Univ. Bremen, Bremen, Germany, 2006.

I. Boyd
Associate Editor